Journal of Materials Chemistry C

Accepted Manuscript

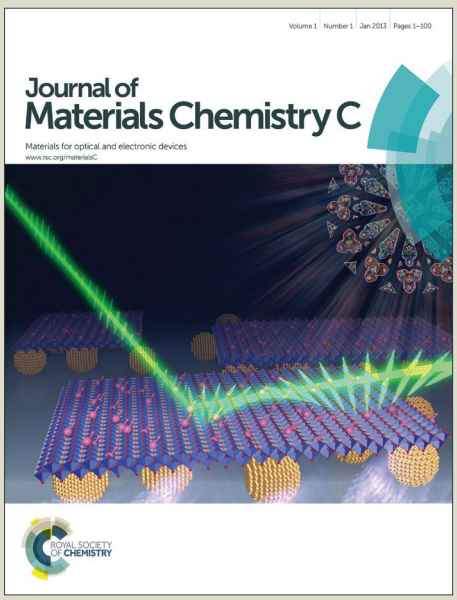

ROYAL SOCIETY OF CHEMISTRY

www.rsc.org/materialsC

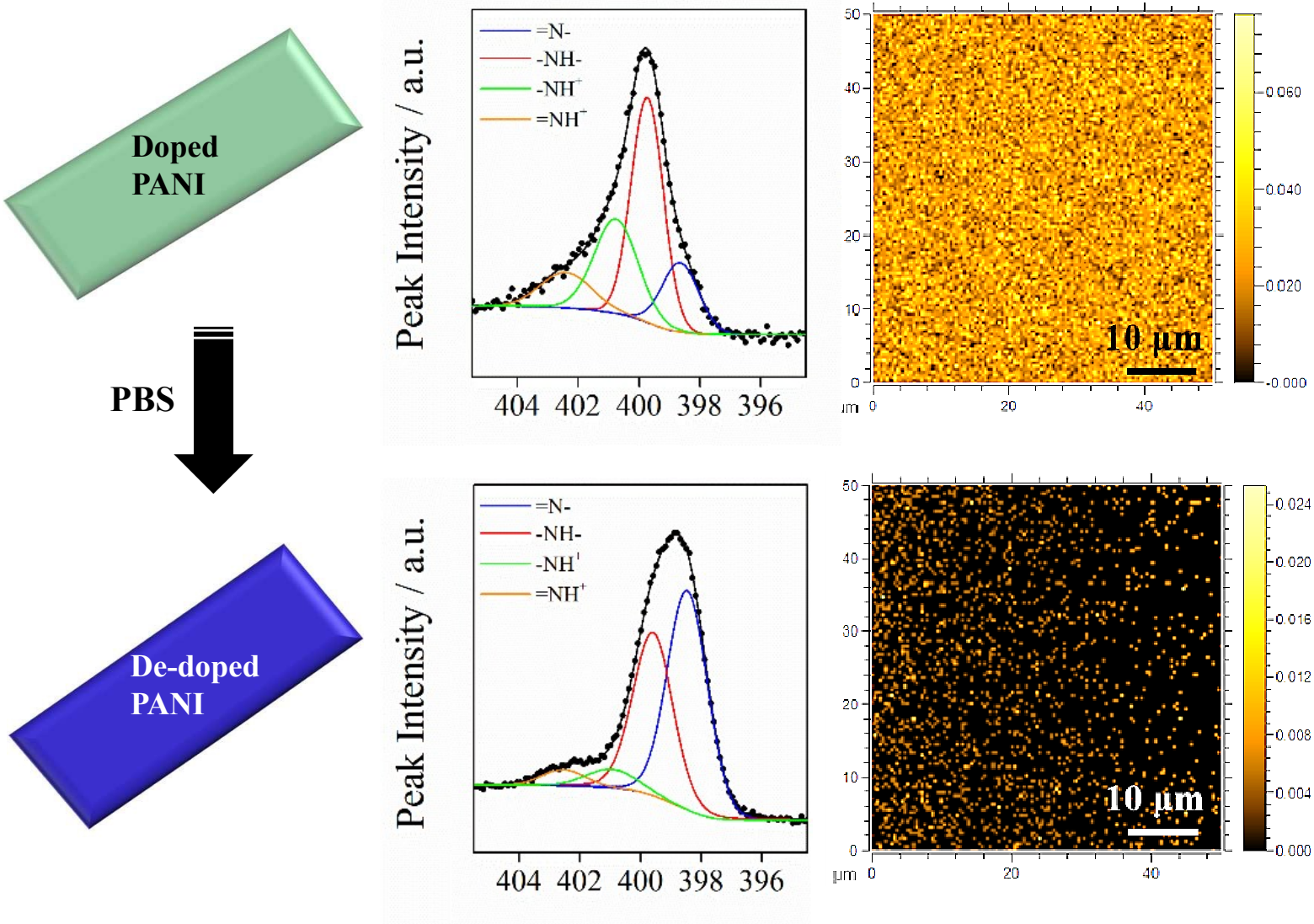

Journal of Materials Chemistry C

RSCPublishing

ARTICLE

Elucidating the deprotonation of polyaniline films by X-ray photoelectron spectroscopy

Cite this: DOI: 10.1039/x0xx00000x

Muzamir M. Mahat,[abc] Damia Mawad,[abc] Geoffrey W. Nelson,[a] Sarah Fearn,[a] Robert G. Palgrave,[d] David J. Payne,[a*] and Molly M. Stevens[abc*]

Received 00th March 2015,
Accepted 00th March 2015

DOI: 10.1039/x0xx00000x

www.rsc.org/MaterialsC

Spin-coated polyaniline (PANI) thin films can be made conductive following treatment with a dopant (reducing or oxidising agent). However, de-doping results in loss of electrical properties. We chemically doped PANI films using *p*-toluene sulfonic acid (*p*TSA) and camphor sulfonic acid (CSA) and examined their ability to retain these dopants and their conductive properties in physiological media. Changes in the protonation level of these films were assessed by N 1s core line spectra in X-ray photoelectron spectroscopy (XPS). PANI films were found to de-dope with a decrease in the ratio of N 1s photoelectron signal corresponding to positively charged nitrogen (i.e. $-NH_2^+$, $=NH^+$) to the total N 1s signal. De-doping of PANI films was confirmed by depletion of the dopant fragment ($-SO_3^-$) as determined from both XPS and atomic distribution in Time-of-Flight Secondary Ion Mass Spectrometry (ToF-SIMS) images. XPS has been successfully used as a tool to elucidate the deprotonation of PANI films and the loss of the dopant from the bulk.

1. Introduction

Intrinsically conducting polymers (CPs) such as polypyrrole (Ppy), polyaniline (PANI) and polythiophene are synthetic polymers that exhibit special chemical, optical and electronic properties. As such, these polymers have been investigated for a wide range of applications such as solar cells,[1] biochemical[2] and electrochemical[3] sensors, electronic circuits[4] and tissue engineering.[5] One of their advantages is that they could be made conductive by simply treating them with a reducing or oxidising agent (dopant). However, this mode of doping is a reversible process, depending on the environmental conditions. For instance, de-doping (loss of dopant) could occur in physiological conditions (pH=7.4, 37 °C), leading to loss of electrical properties.[6] Unfortunately, the de-doping of CPs and its quantitative characterisation has been largely overlooked in the biomedical field. Therefore, there is a need for an in depth analysis of the changes that occur in the oxidation state of the CPs and the level of doping following incubation in biologically relevant conditions. We herein use X-ray photoelectron spectroscopy (XPS) as a robust tool to probe these changes both on the surface and in the bulk of conductive PANI films.

We chose PANI as a model system due its controllable electrical conductivity,[7] unique redox properties,[8] and ease of processing into films. PANI films are extensively used in a range of bio-applications including bio-sensors,[9,10] as a coating material for medical devices[11] and as polymeric platforms for culturing different cell lines such as PC-12 pheochromocytoma ,[12] neural,[13] and cardiomyocyte cells[14] with demonstrated biocompatibility. PANI can exist in a number of different oxidation states; however the emeraldine base (EB) is of particular interest because it could be converted to the conductive form of PANI, the emeraldine salt (ES) (see Fig. 1), by simply mixing it with small acid molecules such as camphor sulfonic acid (CSA),[15] *p*-toluene sulfonic acid (*p*TSA),[16] dodecylbenzenesulfonic (DBSA),[17] hydrochloric acid (HCl)[18] and perchloric acid ($HClO_4$).[19]

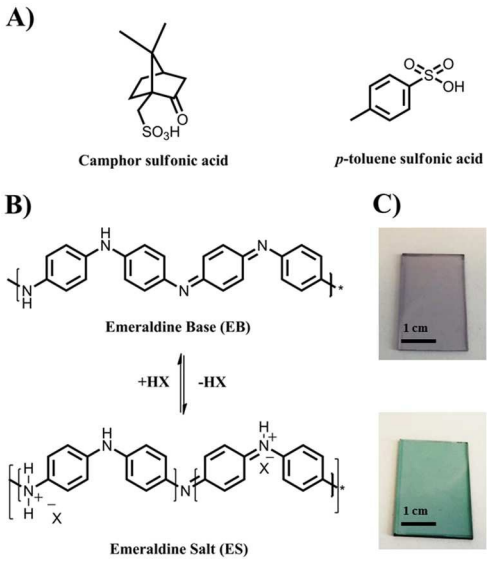

Fig.1 A) Chemical structures of dopants. **B)** Doping mechanism of PANI emeraldine base (EB) with acids (HX) to convert it into the conductive form, PANI emeraldine salts (ES). **C)** Thin films of undoped (blue) and doped (green) PANI.

These acids protonate the amine and/or imine, resulting in positively charged nitrogen.[8] To maintain electroneutrality of the polymeric backbone, the negatively charged counter-ions such as $-SO_3^-$ in *p*TSA, DBSA, CSA or Cl^- and ClO_4^- in HCl and $HClO_4$ bind either ionically to the positively charged nitrogen[20] or *via* ring-attachment to backbone phenyl groups.[21-23] Any change in their interaction with the polymeric backbone leads to a drop in conductivity and variation in oxidation state of the polymer.

It has been reported that PANI deprotonates at physiological pH (7.4), thus losing its conductivity due to leaching out of the dopant.[6] The pH of PBS (7.4) is higher than the pKa of imine (5.5) and amine (2.5) groups, therefore during incubation deprotonation of these groups occurs. This is a major limitation that restricts the potential use of PANI in regenerative medicine applications and impinges its function in both the monitoring of biological processes and the stimulation of cells.[24] While there are few studies investigating how to improve the stability of PANI in the doped state by using large negatively charged polyelectrolyte such as polyacrylic acid (PAA)[25] and polystyrene sulfonate acid (PSS),[26] the majority of previous research has focussed on small acid molecule dopants.[27-29]

Applied to CP, XPS has been shown to be a powerful technique for investigating the nature of the polymeric cation, its interaction with the dopant counter ion, and the structural disorder in these electrically conductive polymers.[30] It has been used to reveal the elemental composition and oxidation states, and also investigate changes on the surface of PANI either post-surface modification,[31] or following doping/protonation.[32] XPS has been extensively utilised to reveal the protonation level of PANI films at fabrication.[31,33,34] The N 1s core level has served as a prime determinant of the extent of protonation in PANI through careful analysis of the core level line shape.[8,35] It has been reported that the N 1s components at 401.1 eV and 402.2 eV are attributed to protonated amine and protonated imine, respectively.[20,34,36] Monitoring the area ratio of these two peaks to the total area of the N 1s spectrum reveals the doping/de-doping percentage (known as the 'level of doping/de-doping level');[34] this value can be used to monitor and quantify the de-doping mechanism that occurs in PANI following incubation in physiological conditions. In a study by Gill *et al.,*[37] XPS measurements were conducted to reveal the stability of PANI composites in physiological conditions for up to 96 hours but did not provide either detailed quantification of the level of doping or an analysis of the dopant chemical composition.

Although the surface layer of the PANI film is first to be exposed to any media, the bulk may also be chemically changed. Depth analysis by XPS can provide such information and has successfully been performed for polymeric materials.[38,39] Nobuta and Ogawa studied the changes of the chemical states of C 1s spectra through the depth for different types of polymers structure such as aliphatic polymers, aromatic polymers, fluorine containing polymers, and natural polymers.[38] Gilbert *et al.*,[39] investigated the multilayers of polyelectrolytes and revealed the inter layer diffusivity of chitosan in [poly(acrylic acid)/poly(ethylene oxide)] (PAA/PEO) films. These authors also tested the effect of chitosan diffusivity when a blocking layer is present. Through their depth analysis, the displacement of PEO films by chitosan has been shown by monitoring the decrease in signal intensity of the C 1s core level. Zhang *et al.*[40] conducted an XPS analysis of multilayered PANI films measured at different take off angles (90° and 15°). The grazing emission (15°) measurements indicated higher elemental compositions of PANI films (carbon and nitrogen) than the normal emission measurements (90°). However, this study only provided the elemental changes, without any investigation regarding the protonation state of PANI.

In this work, we demonstrate the use of XPS to examine and quantify the deprotonation of PANI films upon incubation in physiological conditions. PANI-EB was doped chemically by small molecule dopants: *p*TSA and CSA. PANI thin films were fabricated by spin coating and then incubated in physiological conditions for 0.5 and 24 hours. The changes of protonation level of these films were assessed by N 1s core line spectra in XPS, revealing the doping level of the PANI films surfaces. The core level for sulfur (S 2p) was also studied to determine its stability in binding to the PANI backbone after immersion in buffer. Depth analysis was also conducted in an attempt to monitor changes in the dopant species in the bulk of PANI films. Other characterisation techniques such as ToF-SIMS, and UV-Vis were used to monitor the doping/de-doping of these films.

2. Experimental

2.1 Materials

Polyaniline emeraldine base (PANI-EB, 50 kDa), camphor sulphonic acid (CSA), *p*-toluene sulfonic acid (*p*TSA), and hexaflouro-isopropanol (HFIP) were purchased from Sigma Aldrich (UK) and phosphate buffered saline (PBS, 0.1M) was made from tablets purchased from Life Technologies (UK).

2.2 Fabrication of thin films

Thin films of doped PANI were fabricated by dissolving PANI-EB in HFIP with the respective acid dopant and then spun coated. In a typical procedure**,** 0.3 wt% of PANI–EB (150 mg) and 0.3 wt % *p*TSA or CSA (150 mg) were dissolved in HFIP (50 mL). The solution was centrifuged for 1 hour at 3800 rpm (Centrifuge 5804 R). This step was followed by a filtration process (200 µm filter paper by Merck) to obtain *p*TSA or CSA-doped PANI solutions free of any undissolved particles. The solution of doped PANI was then deposited on glass substrates (20 mm x 50 mm size) using the spin coating technique (Model WS-650SZ-6NPP/LITE, Laurell technologies) at a speed of 800 rpm. Films were dried by nitrogen gas purging at room temperature and stored in the dark until used. PANI without any dopant was also dissolved in HFIP to serve as a control (undoped PANI).

2.3 Incubation in physiological conditions

All samples of PANI films (doped/undoped) were incubated at 37 °C in phosphate buffered saline (PBS, pH 7.4) for 30 minutes or 24 hours. Samples were then washed in deionised water (DI-H_2O) and dried at room temperature. This was followed by characterisation using XPS for surface and depth analysis, and other complementary techniques such as UV-Vis spectroscopy and Time of Flight Mass Spectrometry (ToF-SIMS).

2.4 Characterisation methods

X-ray photoelectron spectroscopy (XPS). XPS spectra were obtained on a Thermo Fisher K-Alpha spectrophotometer utilising a monochromatic Al-Kα X-ray source (Energy = 1486.71 eV). Samples were positioned at the electron take-off angle normal to the surface with respect to the analyser. Survey spectra in the range 0–1300 eV were recorded for each sample (pass energy = 200 eV) followed by high-resolution measurements (pass energy = 50 eV) for C 1s, N 1s, S 2p, and O 1s core levels. XPS spectra were calibrated to the adventitious C1s signal (284.6 eV). Curve fitting was carried out using Thermo Avantage Software (v. 5.948) using a Shirley background. The amine peak was fixed at 399.24 eV, whilst the positions for the other peaks were variable; however, reasonable peak fits had imine, protonated amine, and protonated imine located at ≈ 398 eV, ≈ 400 eV, and ≈ 402 eV, respectively. Curve fits employed pseudo-Voight functions, which are the product of Lorentzian and Gaussian line shapes, with the percentage of the Lorentzian component variable between 0 and 15 %. The full half-width maximum (FHWM) was constrained to be between 1.2 and 2 eV. Peak areas were normalised within Thermo Avantage using atomic sensitivity factors for the Al Kα anode ('AlWagner' library)[41] and from these areas nitrogen composition, the level of doping, and elemental ratios were determined. The S2p region was fit similarly, but with the S $2p_{1/2}$ peak + 1.2 eV higher in binding energy than the S $2p_{3/2}$ and with peak area constrained to one half that of the S $2p_{3/2}$ peak. A low energy electron/ion flood gun was used to ensure effective surface charge compensation. The quantitative determination of the chemical compositions was calculated using methods described by Seah.[42] Depth-profiling was conducted using an EX06 Argon Ion Source to sputter samples at an estimated rate of 0.21 nm/s. This was determined by total depletion of polymers films with thickness of ~73 nm (see Table S2). After various time intervals, 'snapshots' of the relevant core level spectra were obtained (acquired by holding the analyser voltage constant and using the detector width to sample a binding energy window). These depth-profiles were analysed using CASA XPS (v. 2.3.16).

UV-Vis spectroscopy (UV-Vis). An optical absorption study was carried out using UV-Vis spectrophotometer (Perkin Elmer Lambda 25). Polymer films deposited on glass substrates were placed in a glass cuvette to ease sample handling. A glass substrate without any film deposited was used as the blank sample. The scans were conducted in the range of 300 nm to 900 nm wavelengths with scan speed of 480 nm/s.

Time of Flight Secondary Ion Mass Spectrometry (ToF-SIMS). The distribution of the dopant on the surface was monitored by TOF-SIMS using an IONTOF ToF SIMS V instrument, equipped with bismuth liquid metal ion source (LMIS) pulsed gun incident at 45°. A 25 keV Bi^+ primary ion beam of 1 pA current was used to generate the secondary ions using the high current bunched mode for high mass resolution mass spectroscopy. For ion mapping, the primary ion beam was used in the burst alignment mode to obtain high lateral resolution during the analysis. In this study, ion maps showing the distribution of the dopant element on the surface were obtained for an area of 50 µm x 50 µm.

3. Results and discussion

3.1 XPS Analysis

The atomic surface compositions of all PANI films were first analysed from high-resolution spectra of the main components: carbon, nitrogen, oxygen, and sulfur (see Fig. S1 and Table S1). The changes in the protonation states of PANI films were monitored through the N 1s core level spectra (see Fig. 2 and Table 1). These spectra could be fitted into four main chemical states due to the different chemical environments present. These are imine (=N-) at 398.5 eV, amine (-NH-) at 399.5 eV, protonated amine ($-NH_2^+$) at 401.1 eV and protonated imine ($=NH^+$) at 402.2 eV.[20, 34, 36]

As shown in Fig. 2A and Table 1, undoped PANI has a near 1:1 ratio between amine and imine groups, characteristic of the emeraldine base (EB) form of PANI (Fig. 1). The small percentage of protonated nitrogen (~17.7%) is not unexpected.[35] Following incubation in PBS for up to 24 hours, undoped PANI displayed chemical stability without significant changes in its protonation state.

PANI was doped successfully by the small acids *p*TSA and CSA as shown by the increase of protonated amine and protonated imine peaks (see Fig. 2B and Fig. 2C). However, unprotonated imine signal remains, suggesting the incomplete doping of the PANI film. Both small acid dopants lead to similar doping levels; 22.5% and 29.2% for *p*TSA and CSA, respectively. After incubation in PBS, evidence for the deprotonation of both *p*TSA and CSA doped PANI films was seen in Fig. 2B and Fig. 2C, respectively. Both protonated imine and protonated amine composition decreased as a function of increased incubation time.

The doping level (the contribution of all N^+ species to the total nitrogen content) after incubation was quantified.[34] (see Table 1). *p*TSA doped PANI exhibited a significant drop in its protonation level from 22.5% to 13.3% after 24 hours in PBS. Similar trends were observed for CSA-PANI films with only 18.4% protonation remaining after 24 hours. From this we conclude that deprotonation has occurred in both types of films after 30 minutes and 24 hours incubation in PBS (pH = 7.4).

Table 1 The ratio of nitrogen species to total nitrogen content, level of doping and the ratio of S $2p_{3/2}$ / N 1s.

Film	Incubation Time (hours)	=N-	-NH-	$-NH_2^+$	$=NH^+$	Level of Doping (%)	S $2p_{3/2}$/N 1s
Undoped PANI	0	0.48	0.34	0.12	0.06	17.7	-
	0.5	0.42	0.38	0.14	0.06	20.1	-
	24	0.54	0.28	0.12	0.06	17.4	-
*p*TSA doped PANI	0	0.32	0.46	0.14	0.08	22.5	0.66
	0.5	0.30	0.51	0.15	0.04	18.7	0.004
	24	0.50	0.37	0.08	0.05	13.3	0.001
CSA doped PANI	0	0.36	0.34	0.19	0.10	29.2	0.28
	0.5	0.42	0.46	0.10	0.04	14.5	0.008
	24	0.33	0.44	0.15	0.08	18.4	0.005

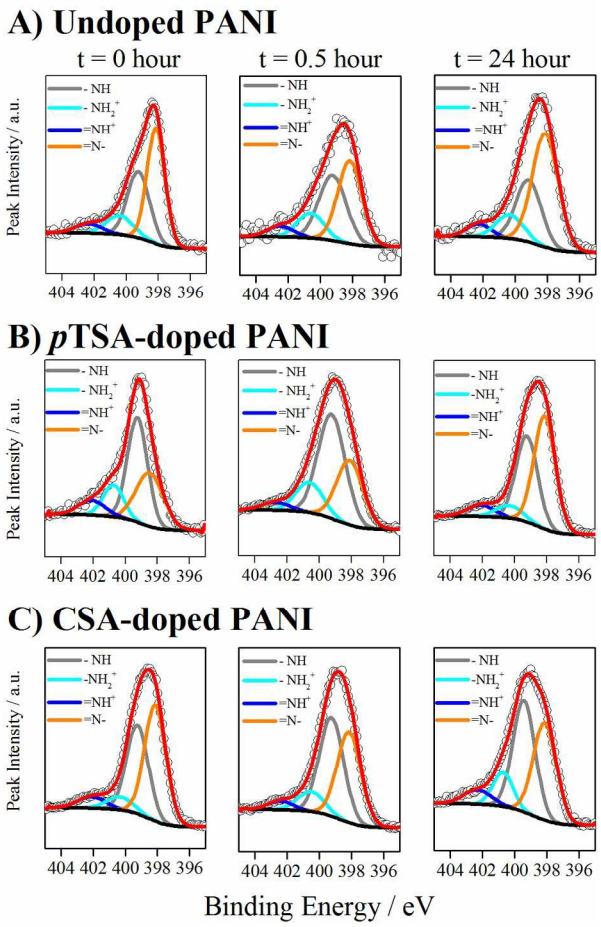

Fig. 2 High resolution of N 1s core line spectra of: **A)** undoped PANI, **B)** *p*TSA and **C)** CSA-doped PANI in different incubations times.

This de-doping mechanism has been observed by Wang *et al.*[43] who reported that small anion dopants can diffuse out of PANI films. The pH of PBS is higher than the pKa of imine and amine groups, therefore during incubation it is expected that deprotonation of these groups occurs. Indeed, this is observed post incubation for all samples, as evidenced by reduction of photoelectron signal associated with $=NH^+$- and $-NH_2^+$- species.

To confirm that the decrease in the protonation level is related to the loss of the dopant, we monitored the sulfur content of the films by XPS and quantified its ratio to nitrogen (S 2p/N 1s). As listed in Table 1, the ratio decreased as incubation time increased. This observation is unambiguous in Fig. 3, which shows the almost negligible S 2p signal after only 30 minutes of incubation in PBS.

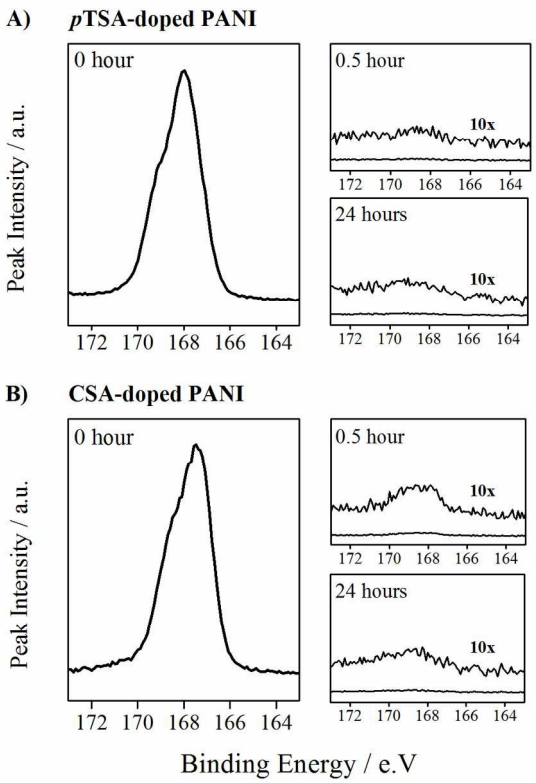

Fig. 3 High resolution S 2p spectra of the surfaces of **(A)** *p*TSA and **(B)** CSA-doped PANI films as function of different incubation times. The spectra for incubated films have been multiplied 10 times to highlight the small residual S 2p signal. All data are plotted on the same arbitrary y-axis as the 0 hour spectra.

These results were in agreement with the observed drop in the protonated species. Therefore, it is clear that both small acid dopants are diffusing out of PANI during short and prolonged incubation in PBS.

We next conducted a depth analysis of the doped PANI films to monitor the presence of sulfur in the bulk of the film. At fabrication, the S 2p depth profiles for *p*TSA and CSA doped PANI in Fig. S2 show evidence for two chemical environments of sulfur. The S 2p signal at higher binding energy for un-sputtered *p*TSA PANI is assigned to sulfur within ring-attached mono-substituents such as $-SO_3^-$ (≈ 167.3 eV) and $-SO_3H$ (≈ 168.5 eV).[21] A species of low binding energy was observed (≈ 164 eV) which is most likely a result of the monoatomic Ar^+ sputtering during depth profiling leading to reduced sulfur species being generated. It remains a challenge to monitor/perform depth analysis on sensitive polymeric systems.[38] Although quantitative analysis is not feasible, it is possible to qualitatively state that sulfur is present throughout the film; it only disappears after sputtering to the glass substrate (etch time > 640 sec). In contrast in the incubated films, sulfur was not present at the surface, near-surface and the bulk (see Fig. S2). This result confirmed the diffusion and loss of the dopant, which accounts for the observed deprotonation. The loss of dopant from PANI films subject to water has been reported using other techniques such as quartz crystal microbalance[44] or by monitoring the drop in the electroactivity of PANI films in buffer pH > 4.5.[43] Additionally, the deprotonation and loss of conductivity has been shown for thicker films (50-100 μm) incubated in PBS.[37] Our study presents the use of XPS as an alternative technique for monitoring and quantifying the ratio of the dopant in PANI films subject to physiological conditions. We conclude that neither of the two small acid molecules dopants is caRTHpable of surviving even 30 minutes of incubation in PBS (vide supra). Alternative dopants must be sought to achieve this feat.

3.2 UV-Vis spectra

To investigate the effect of PBS on the electronic structure of the PANI films, UV-Vis spectra were measured. Undoped PANI films showed the characteristic spectral features at the wavelengths of 345 nm and 592 nm (see Fig. S3), which represented the benzoid and quinoid segments of PANI, respectively.[45] Following incubation in PBS for 24 hours, no change was observed as expected. At fabrication, *p*TSA and CSA-doped PANI (Fig. 4A and Fig. 4B) showed three spectral features at the wavelengths of 350 nm, 450 nm and 815 nm. These peaks correspond to the emeraldine salt form of PANI, thus confirming that doping by those acids was successful.[45] Upon incubation in physiological media for 24 hours, the peak at 450 nm disappeared while the peak at 815 nm shifted to 610 and 645 nm for *p*TSA and CSA-doped PANI respectively. These spectra are similar to the undoped PANI, confirming that the doped PANI films have been deprotonated in buffer pH=7.4, in agreement with the XPS data.

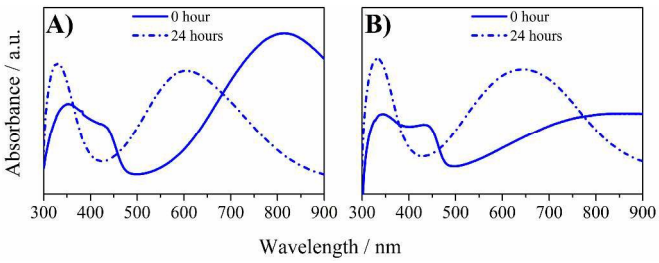

Fig. 4 UV-Vis spectra of: **A)** *p*TSA and **B)** CSA-doped PANI films before and after incubation in physiological conditions. Solid line represents doped PANI and dotted line represents the spectra of films post-24 hours incubation.

3.3 ToF-SIMS

ToF-SIMS has been used in characterising the atomic distribution of polymeric materials.[46] We have used this technique to probe the distribution of the sulfonic acid fragment ($-SO_3^-$) of the dopant on the surface of PANI films. This fragment binds to the positively charged nitrogen in the PANI backbone. As revealed in Fig. 5A and Fig. 5B, the dopant appears to be homogeneously distributed on the surface of the films at fabrication.

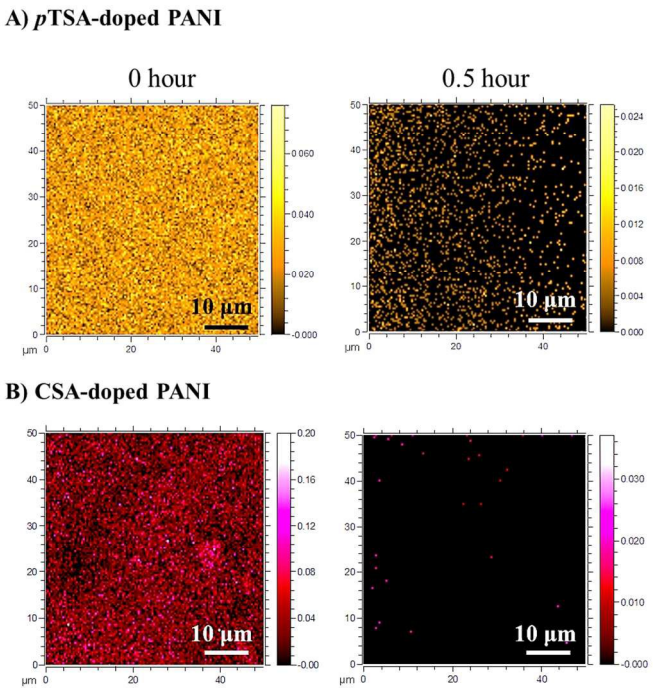

Fig. 5 ToF-SIMS images (normalised to the total counts) revealing the distribution of SO_3^- on **(A)** *p*TSA and **(B)** CSA-doped PANI films at fabrication and after 0.5 hour incubation in buffer.

Post-incubation in physiological conditions, the dopant fragment was depleted, supporting the XPS findings. This is due to the deprotonation of the positively charged nitrogen, which consequently leads to loss in the ionic interaction of the negatively charged dopant fragment $–SO_3^-$.

Conclusions

XPS was successfully used as a tool to quantify the deprotonation of doped-polyaniline films (by CSA and *p*TSA) in physiological conditions. Both surface and depth analysis revealed the loss of dopant following incubation in PBS, which converted the films from a protonated to non-protonated form. TOF-SIMS has been also used as a characterisation technique to monitor the distribution of the counter-ion on the surface. The obtained results were in agreement with the XPS data that revealed depletion of sulfur following incubation in buffer. To confirm these results, a well-established technique for the characterisation of conducting polymer electronic states, UV-Vis spectrophotometry, was used. Spectra recorded before and after incubation clearly showed a shift from the ES to the EB form of PANI. We herein have presented an in depth study using XPS as a robust tool to monitor changes in oxidation state of PANI and the dopant, as well as quantify the loss of dopant and decrease in protonation level post-incubation. This was complimented by TOF-SIMS as a technique to probe changes in elemental composition on the surface. As the findings of this study showed the depletion of the dopant following incubation in biologically relevant conditions, there is an urgent need for more stable dopants to be used, which can include large molecular weight polyelectrolytes or small dopants consisting of multivalent anions capable of ionically crosslinking with positively charged backbones of conducting polymers.

Acknowledgements

M.M.M. would like to thank the Public Service Department of Malaysia for the PhD scholarship via King of Malaysia scheme and University Teknologi MARA (UiTM). D.M. is gratefully funded by the Marie Curie International Incoming Fellowship under grant agreement no. 328897. We acknowledge Miss Emily Glover (UCL) for help with performing XPS experiment. D.J.P. acknowledges support from the Royal Society (UF100105). D.J.P. and R.G.P. acknowledge the support of the Materials Design Network.

Notes

[a] Department of Materials, Imperial College London, Exhibition Road, London SW7 2AZ, United Kingdom
[b] Department of Bioengineering, Imperial College London, Exhibition Road, London SW7 2AZ, United Kingdom
[c] Institute of Biomedical Engineering, Imperial College London, Exhibition Road, London SW7 2AZ United Kingdom.
[d] Department of Chemistry, University College London, 20 Gordon Street, London WC1H 0AJ, United Kingdom

†Electronic Supplementary Information (ESI) available: [details of any supplementary information available should be included here]. See DOI: 10.1039/b000000x/

References

1 K. Kawata, S.-N. Gan, D. T.-C. Ang, K. P. Sambasevam, S.-W. Phang and N. Kuramoto, *Polym. Compos.*, 2013, **34**, 1884.
2 B. Thakur, C. A. Amarnath, S. H. Mangoli and S. N. Sawant, *Sensors Actuat. B-Chem.*, 2015, **207**, Part A, 262.
3 W. Kit-Anan, A. Olarnwanich, C. Sriprachuabwong, C. Karuwan, A. Tuantranont, A. Wisitsoraat, W. Srituravanich and A. Pimpin, *J. Electroanal. Chem.*, 2012, **685**, 72.
4 Y. G. Ko, T. G. Do, H. C. Oh, H. J. Lee, H.-G. Han, C. H. Kim and U. S. Choi, *Sci. Rep.*, 2014, **4,** 6655.
5 D. Mawad, E. Stewart, D. L. Officer, T. Romeo, P. Wagner, K. Wagner and G. G. Wallace, *Adv. Funct. Mater.*, 2012, **22**, 2692.
6 P. R. Bidez, S. Li, A. G. Macdiarmid, E. C. Venancio, Y. Wei and P. I. Lelkes, *J. Biomat. Sci. Polym. Ed.*, 2006, **17**, 199.
7 Y. Liao, V. Strong, W. Chian, X. Wang, X.-G. Li and R. B. Kaner, *Macromolecules*, 2012, **45**, 1570.
8 E. T. Kang, K. G. Neoh and K. L. Tan, *Prog. Polym. Sci.*, 1998, **23**, 277.
9 P. Lin and F. Yan, *Adv. Mater.*, 2012, **24**, 34.
10 T. Ahuja, I. A. Mir, D. Kumar and Rajesh, *Biomaterials*, 2007, **28**, 91.
11 P. K. Prabhakar, S. Raj, P. R. Anuradha, S. N. Sawant and M. Doble, *Colloids Surf. B: Biointerfaces*, 2011, **86**, 146.
12 H. J. Wang, L. W. Ji, D. F. Li and J.Y. Wang, *J. Phys. Chem. B*, 2008, **112**, 2671.
13 L. Ghasemi-Mobarakeh, M. P. Prabhakaran, M. Morshed, M. H. Nasr-Esfahani, H. Baharvand, S. Kiani, S. S. Al-Deyab and S. Ramakrishna, *J. Tissue Eng. Regen. Med.*, 2011, **5**, e17.
14 A. Borriello, V. Guarino, L. Schiavo, M. A. Alvarez-Perez and L.

Ambrosio, *J. Mater. Sci: Mater. Med.*, 2011, **22**, 1053.
15 Y. Zhou, Y. Wang, D. He, C. Ju, Q. Gao, L. Gao and M. Fu, *J. Nanosci. Nanotechnol.*, 2014 **14**, 3417.
16 M. O. Ansari, M. M. Khan, S. A. Ansari, I. Amal, J. Lee and M. H. Cho, *Chem. Eng. J.*, 2014, **242**, 155.
17 D. Nithyaprakash, J. Chandrasekaran, B. Punithaveni and L. Sasikumar, *Optik*, 2014, **125**, 5343.
18 D. Geethalakshmi, N. Muthukumarasamy and R. Balasundaraprabhu, *Optik*, 2014, **125**, 1307.
19 A. Saraswat, L. K. Sharma, S. Singh and R. K. P. Singh, *Synth. Met.*, 2013, **167**, 31.
20 E. T. Kang, K. G. Neoh, S. H. Khor, K. L. Tan and B. T. G. Tan, *Polymer*, 1990, **31**, 202.
21 X. L. Wei, M. Fahlman and A. J. Epstein, *Macromolecules*, 1999, **32**, 3114.
22 J. Yue and A. J. Epstein, *Macromolecules*, 1991, **24**, 4441.
23 J. Yue, Z. H. Wang, K. R. Cromack, A. J. Epstein and A. G. MacDiarmid, *J. Amer. Chem. Soc.*, 1991, **113**, 2665.
24 N. K. Guimard, N. Gomez and C. E. Schmidt, *Prog. Polym. Sci.*, 2007, **32**, 876.
25 S. A. Chen and H. T. Lee, *Macromolecules*, 1995, **28**, 2858.
26 S. J. Yoo, J. Cho, J. W. Lim, S. H. Park, J. Jang and Y.-E. Sung, *Electrochem. Commun.*, 2010, **12**, 164.
27 S. N. Bhadra and N. K. Singha and D Khastgir., *Polym. Int.*, 2007, **56**, 919.
28 N. Menegazzo, D. Boyne, H. Bui, T. P. Beebe and K. S. Booksh, *Anal. Chem.*, 2012, **84**, 5770.
29 G. D. Khuspe, S. T. Navale, M. A. Chougule and V. B. Patil, *Synth. Met.*, 2013, **185–186**, 1.
30 L. Atanasoska, K. Naoi and W. H. Smyrl, *Chem. Mater.*, 1992, **4**, 988.
31 E. T. Kang, K. G. Neoh, K. L. Tan, Y. Uyama, N. Morikawa and Y. Ikada, *Macromolecules*, 1992, **25**, 1959.
32 E. T. Kang, K. G. Neoh and K. L. Tan, *Surf. Interface Anal.*, 1992, **19**, 33.
33 D. Wei, A. Pivrikas, H. Karhu, H. S. Majumdar, T. Lindfors, C. Kvarnstrom, R. Osterbacka and A. Ivaska, *J. Mater. Chem.*, 2006, **16**, 3014.
34 S. Golczak, A. Kanciurzewska, M. Fahlman, K. Langer and J. J. Langer, *Solid State Ionics*, 2008, **179**, 2234.
35 E. T. Kang, K.G. Neoh and K. L. Tan, *Synth. Met.*,1995, **68**, 141.
36 Y. Chen, E. T. Kang, K. G. Neoh, S. L. Lim, Z. H. Ma and K. L. Tan, *Colloid Polym. Sci.*, 2001, **279**, 73.
37 E. Gill, A. Arshak, K. Arshak and O. Korostynska, *Sensors*, 2007, **7**, 3329.
38 T. Nobuta and T. Ogawa, *J. Mater. Sci.*, 2009, **44**, 1800.
39 J. B. Gilbert, M. F. Rubner and R. E. Cohen, *Proc. Natl. Acad. Sci. U. S. A.*, 2013, **110**, 6651.
40 J. Zhang, D. P. Burt, A. L. Whitworth, D. Mandler and P. R. Unwin, *PCCP.*, 2009, **11**, 3490.
41 C. D. Wagner, L. E. Davis, M. V. Zeller, J. A. Taylor, R. M. Raymond and L. H. Gale, *Surf. Interface Anal.,* 3. 211 (1981) and are reproduced here from Appendix 6 of *"Practical Surface Analysis", Vol. 1., 2nd Edition, by C. D. Wagner, eds. D. Briggs and M.P. Seah, Published by J. Wiley and Sons in 1990, ISBN 0-471-92081-9*
42 M.P. Seah. "Quantification of AES and XPS" In: D. Briggs, *Practical surface analysis by Auger and X-ray photoelectron spectroscopy*, John Wiley & Son Ltd., 1990, pp: 223-251.
43 Y. Wang and K. Levon, *Macromol. Symp.*, 2012, **317-318**, 240.
44 M. M. Ayad and E. A. Zaki, *Eur. Polym. J.*, 2008, **44**, 3741.
45 J. Tarver, J. E. Yoo, T. J. Dennes, J. Schwartz and Y-L. Loo, *Chem. Mater.,* 2009, **21**, 280.
46 A. Benninghoven, *Angew. Chem. Int. Ed.*, 1994, **33**, 1023.